Applied Mathematics and Computation 218 (2011) 1941–1961

Contents lists available at ScienceDirect

Applied Mathematics and Computation

journal homepage: www.elsevier.com/locate/amc

Qualitative study of a quarantine/isolation model with multiple disease stages

Mohammad A. Safi, Abba B. Gumel *

Department of Mathematics, University of Manitoba, Winnipeg, Manitoba, Canada R3T 2N2

ARTICLE INFO

Keywords:
Quarantine/isolation
Equilibria
Reproduction number
Stability
Gamma distribution

ABSTRACT

Recent studies suggest that, for disease transmission models with latent and infectious periods, the use of gamma distribution assumption seems to provide a better fit for the associated epidemiological data in comparison to the use of exponential distribution assumption. The objective of this study is to carry out a rigorous mathematical analysis of a communicable disease transmission model with quarantine (of latent cases) and isolation (of symptomatic cases), in which the waiting periods in the infected classes are assumed to have gamma distributions. Rigorous analysis of the model reveals that it has a globally-asymptotically stable disease-free equilibrium whenever its associated reproduction number is less than unity. The model has a unique endemic equilibrium when the threshold quantity exceeds unity. The endemic equilibrium is shown to be locally and globally-asymptotically stable for special cases. Numerical simulations, using data related to the 2003 SARS outbreaks, show that the cumulative number of disease-related mortality increases with increasing number of disease stages. Furthermore, the cumulative number of new cases is higher if the asymptomatic period is distributed such that most of the period is spent in the early stages of the asymptomatic compartments in comparison to the cases where the average time period is equally distributed among the associated stages or if most of the time period is spent in the later (final) stages of the asymptomatic compartments. Finally, it is shown that distributing the average sojourn time in the infectious (asymptomatic) classes equally or unequally does not effect the cumulative number of new cases.

1. Introduction

Since the pioneering works of Sir Ronald Ross, Kermack and McKendrick (see, for instance, [15,16,23]), numerous mathematical models have been designed and used to gain insight into transmission dynamics of emerging and re-emerging diseases of public health interest. The models, typically of the forms of deterministic or stochastic systems of non-linear differential equations, are used to evaluate various control strategies such as: vaccination, the use of antibiotics or antivirals, quarantine, isolation, etc. Of the aforementioned control strategies, the use of quarantine (of individuals suspected of being exposed to the disease) and isolation (of those with clinical symptoms of the disease) are the most commonly used (since the beginning of recorded human history). These measures have been used in the control of numerous diseases such as leprosy, plague, cholera, typhus, yellow fever, smallpox, diphtheria, tuberculosis, measles, ebola, pandemic influenza and, more recently, severe acute respiratory syndrome (SARS) [3,11,18–20,22,29,31,32]. Furthermore, quarantine and isolation are popularly applied to combat the spread of animal diseases such as bovine tuberculosis, rinderpest, foot-and-mouth, psittacosis,

* Corresponding author.
E-mail address: gumelab@cc.umanitoba.ca (A.B. Gumel).

0096-3003/$ - see front matter
doi:10.1016/j.amc.2011.07.007

Newcastle disease and rabies [11,14]. It is known, however, that quarantine and isolation measures, especially in the context of a new emerging disease, are initially not administered effectively, but are gradually refined (as more data and knowledge of the disease transmission process becomes available (see, for instance, [8])).

Numerous mathematical modeling work have been carried out to assess the impact of quarantine and isolation in combatting the spread of the diseases (such as some of the aforementioned modeling studies for SARS). However, many of the models used for assessing the impact of the quarantine and isolation measures tend to be built based on the assumption that the disease stages are exponentially distributed. However, some recent studies [7,30] show that it is more realistic to use gamma distribution assumption for the waiting time in the disease stages (rather than exponential distribution assumption). Furthermore, Feng et al. [7] showed that quarantine and isolation models that assume exponential distribution (for the disease stages) may not be suitable for diseases with relatively long latent and/or infectious periods for the case when isolation is not completely effective (i.e., isolated individuals can transmit infection).

The purpose of the current study is to provide a rigorous qualitative analysis of a new deterministic model for transmission dynamics of a communicable disease, subject to the use of quarantine and isolation, where the waiting time in the associated infected classes are assumed to have gamma distribution. The model to be designed extends the SEIQHR model given in [24] by considering multiple stages of the exposed, infectious, quarantined and hospitalized individuals (unlike in [24], it is assumed here that hospitalized individuals do not transmit the infection). Diseases like HIV [25] and influenza [6] are known to have multiple disease (infection) stages.

The paper is organized as follows. The model is formulated in Section 2. The global asymptotic stability of the disease-free equilibrium (DFE) is established in Section 3. The existence of the endemic equilibrium is analyzed in Section 4. Local and global stability proofs for the endemic equilibrium, for special cases, are also provided using a Krasnoselskii sub-linearity trick and a non-linear Lyapunov function of Goh–Voltera type, respectively.

2. Model formulation

The total population at time t, denoted by $N(t)$, is sub-divided into six disjoint classes of susceptible ($S(t)$), exposed ($E(t)$; with m exposed stages), quarantined ($Q(t)$; with m quarantined stages), infectious ($I(t)$; with n infectious stages), hospitalized ($H(t)$; with n hospitalized stages) and recovered ($R(t)$) individuals, so that

$$N(t) = S(t) + \sum_{i=1}^{m} E_i(t) + \sum_{j=1}^{n} I_j(t) + \sum_{i=1}^{m} Q_i(t) + \sum_{j=1}^{n} H_j(t) + R(t).$$

In this paper, unlike in [18], it is assumed that the fraction of infected contacts that can be traced and quarantined at the time of infection is very small. Furthermore, it is assumed that the total population is large in comparison to the size of the infected individuals ($N \gg E + I + Q + H + R$). Consequently, the quarantine of susceptible individuals (feared exposed to the disease) is unlikely to have a significant impact on the disease transmission dynamics. Hence, the quarantine of susceptible individuals is not considered in this study (see also [7]). In other words, in this study, quarantine refers to the isolation of exposed (latently-infected) individuals only.

The susceptible population is increased by the recruitment of individuals into the community (assumed susceptible), at a rate Π. Susceptible individuals may acquire infection, following effective contact with infectious individuals (in any of the n infectious stages) at a rate λ, where

$$\lambda = \frac{\beta \sum_{j=1}^{n} I_j}{N}. \tag{1}$$

It is assumed that infected individuals in the classes E_i, Q_i (with $i = 1,2,\ldots,m$) and H_j (with $j = 1,2,\ldots,n$) do not transmit infection (i.e., it is assumed that exposed individuals do not transmit infection, and that quarantine and isolation measures are implemented in a perfect manner). Although some of these assumptions may not be entirely realistic in some epidemiological settings, such as in the transmission dynamics of influenza (where transmission by infected individuals without disease symptoms occurs), they help in making the mathematical analysis of the resulting large system of non-linear differential equations more tractable. Further, in (1), β is the effective contact rate (contact capable of leading to infection). The population of susceptible individuals is further decreased by natural death (at a rate μ), and increased when recovered individuals lose their infection-acquired immunity (at a rate ψ). Thus, the rate of change of the susceptible population is given by

$$\frac{dS}{dt} = \Pi + \psi R - \lambda S - \mu S.$$

The population of exposed individuals in stage 1 (E_1) is generated by the infection of susceptible individuals (at the rate λ). This population is decreased by progression to the next exposed stage (E_2; at a rate $a_1\alpha$), quarantine (at a rate σ_1) and natural death (at the rate μ), so that

$$\frac{dE_1}{dt} = \lambda S - (a_1\alpha + \sigma_1 + \mu)E_1.$$

The population of exposed individuals in stage i (with $2 \leqslant i \leqslant m$) is generated by the progression of individuals in stage E_{i-1} into the stage i (at a rate $a_{i-1}\alpha$). It is decreased by progression to the next exposed stage (at a rate $a_i\alpha$), quarantine (at a rate σ_i) and natural death (at the rate μ), so that

$$\frac{dE_i}{dt} = a_{i-1}\alpha E_{i-1} - (a_i\alpha + \sigma_i + \mu)E_i; \quad i = 2, \ldots, m.$$

The population of infectious individuals in stage 1 is generated when exposed individuals in the final (m) stage develop symptoms (at the rate $a_m\alpha$). It is decreased by progression to the next infectious stage (I_2; at a rate $d_1\kappa$), hospitalization (at a rate ϕ_1), natural death (at the rate μ) and disease-induced death (at a rate δ_1). This gives

$$\frac{dI_1}{dt} = a_m\alpha E_m - (d_1\kappa + \phi_1 + \mu + \delta_1)I_1.$$

The population of infectious individuals in stage j (with $2 \leqslant j \leqslant n$) is generated by progression of individuals in stage $j-1$ (at a rate $d_{j-1}\kappa$). It is decreased by progression to the next infectious stage (at a rate $d_j\kappa$), hospitalization (at a rate ϕ_j), natural death (at the rate μ) and disease-induced death (at a rate δ_j). Individuals in the final (n) stage of infectiousness recover (at a rate $\gamma_1 = d_n\kappa$). Thus,

$$\frac{dI_j}{dt} = d_{j-1}\kappa I_{j-1} - (d_j\kappa + \phi_j + \mu + \delta_j)I_j; \quad j = 2, \ldots, n-1,$$

and,

$$\frac{dI_n}{dt} = d_{n-1}\kappa I_{n-1} - (\phi_n + \gamma_1 + \mu + \delta_n)I_n.$$

Exposed individuals in stage 1 are quarantined at the rate σ_1. The population of quarantined individuals in stage 1 is decreased by progression to the next quarantined stage (at a rate $b_1\alpha$) and natural death (at the rate μ). Thus,

$$\frac{dQ_1}{dt} = \sigma_1 E_1 - (b_1\alpha + \mu)Q_1.$$

Similarly, the population of quarantined individuals in stage i (with $2 \leqslant i \leqslant m-1$) is generated by the quarantine of exposed individuals in stage E_i (at the rate σ_i) and the progression of quarantined individuals in stage Q_{i-1} into the stage Q_i (at a rate $b_{i-1}\alpha$). It is decreased by progression to the next quarantined stage (at a rate $b_i\alpha$) and natural death (at the rate μ). Thus,

$$\frac{dQ_i}{dt} = \sigma_i E_i + b_{i-1}\alpha Q_{i-1} - (b_i\alpha + \mu)Q_i; \quad i = 2, \ldots, m.$$

It should be mentioned that the parameters σ_i ($i = 1,2,\ldots,m$) can be used to model progressive refinement of quarantine measures in the population, by assuming smaller values of σ_i at the beginning and higher rates for later stages (e.g., for $m = 3$, we can assume smaller values for σ_1 and σ_2, but a higher value for σ_3; i.e., $\sigma_1 < \sigma_2 < \sigma_3$).

The population of hospitalized individuals in stage 1 is generated by the hospitalization of quarantined individuals in the final stage (m; at the rate $b_m\alpha$) and infectious individuals in stage 1 (at the rate ϕ_1). It is decreased by progression to the next hospitalized stage (at a rate $c_1\kappa$), natural death (at the rate μ), and disease-induced death (at a rate δ_{n+1}). Thus,

$$\frac{dH_1}{dt} = b_m\alpha Q_m + \phi_1 I_1 - (c_1\kappa + \mu + \delta_{n+1})H_1.$$

The population of hospitalized individuals in stage j (with $2 \leqslant j \leqslant n$) is generated by the hospitalization of infectious individuals in stage j (I_j) (at the rate ϕ_j) and the progression of hospitalized individuals in stage $j-1$ (H_{j-1}) into the H_j class (at a rate $c_{j-1}\kappa$). It is decreased by the progression to the next hospitalized stage (at a rate $c_j\kappa$), natural death (at the rate μ) and disease-induced death (at a rate δ_{n+j}). Individuals in the final n stage of hospitalized recover (at a rate $\gamma_2 = c_n\kappa$). Thus,

$$\frac{dH_j}{dt} = \phi_j I_j + c_{j-1}\kappa H_{j-1} - (c_j\kappa + \mu + \delta_{n+j})H_j; \quad j = 2, \ldots, n-1,$$

and,

$$\frac{dH_n}{dt} = \phi_n I_n + c_{n-1}\kappa H_{n-1} - (\gamma_2 + \mu + \delta_{2n})H_n.$$

As in the case for the of quarantine measures discussed above, the parameters ϕ_i ($i = 1,\ldots,n$) can also be used to model the progressive refinement of isolation (in hospital; so that, for $n = 3$, we can have $\phi_1 < \phi_2 < \phi_3$). Finally, the population of recovered individuals is generated by the recovery of non-hospitalized and hospitalized infectious individuals in the final n stage (at the rates γ_1 and γ_2, respectively). It is decreased by the loss of natural immunity (at the rate ψ) and natural death (at the rate μ), so that

$$\frac{dR}{dt} = \gamma_1 I_n + \gamma_2 H_n - (\psi + \mu)R.$$

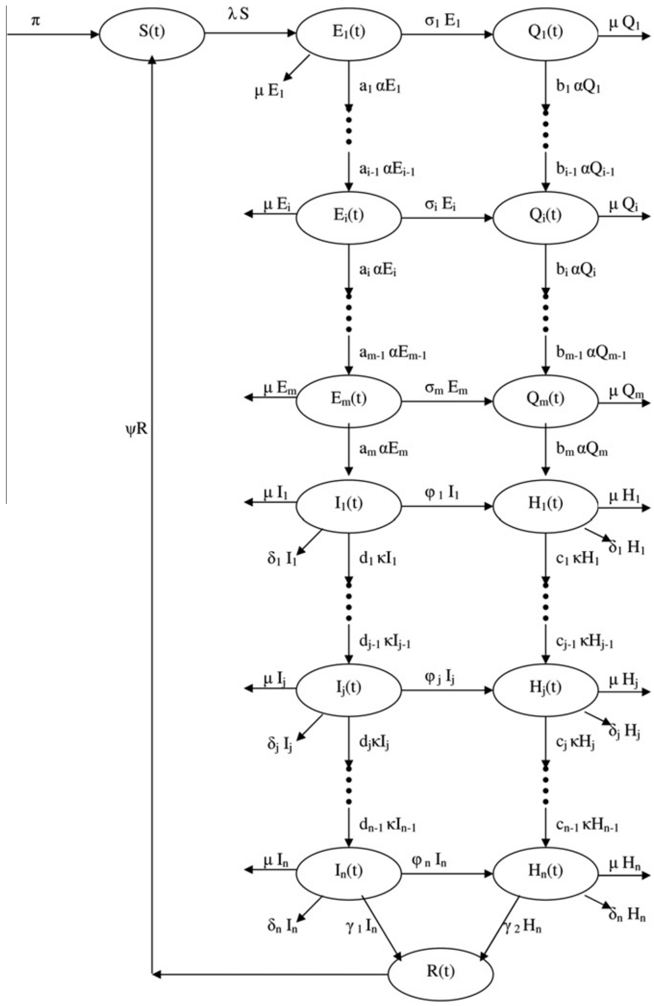

Fig. 1. Flow diagram of the model (6).

It should be stated that, in the above formulation, a_i, b_i, c_j, d_j ($i = 1,2,\ldots,m$; $j = 1,2,\ldots,n$) are constants. Furthermore, it is assumed that the distributions of exposed, quarantined, infectious and hospitalized periods are exponential, given by

$$\begin{aligned} &p_{E_i}(s) = a_i\alpha e^{-a_i\alpha s},\\ &p_{I_j}(s) = d_i\kappa e^{-d_i\kappa s},\\ &p_{Q_i}(s) = b_i\alpha e^{-b_i\alpha s},\\ &p_{H_j}(s) = c_j\kappa e^{-c_j\kappa s} \quad \text{for } i = 1,\ldots,m \quad j = 1,\ldots,n. \end{aligned} \tag{2}$$

In (2), $T_{E_i} = 1/a_i\alpha$, $T_{I_j} = 1/d_j\kappa$, $T_{Q_i} = 1/b_i\alpha$ and $T_{H_j} = 1/c_j\kappa$ are the mean exposed, quarantined, infectious and hospitalized periods, respectively. The relations in (2) are such that:

$$\sum_{i=1}^{m}\frac{1}{a_i\alpha} = \sum_{i=1}^{m}\frac{1}{b_i\alpha} = \frac{1}{\alpha} \quad \text{and} \quad \sum_{j=1}^{n}\frac{1}{c_j\kappa} = \sum_{j=1}^{n}\frac{1}{d_j\kappa} = \frac{1}{\kappa}. \tag{3}$$

That is, the respective mean time spent in a given infected compartment (e.g., $1/\kappa$ for the hospitalized compartment, H) is shared among the various stages in that compartment. In other words, the time period $1/\kappa$ is distributed equally (if $c_1 = c_2 = \cdots = c_n = n$) or unequally (if $c_1 \neq c_2 \neq \cdots \neq c_n \neq n$) between all the H_j ($j = 1,2,\ldots,n$) stages. Hence, this formulation extends the formulation in [7], where these periods are equally distributed among the relevant stages (for all the infected compartments, E, Q, I, H), by allowing for equal or unequal distribution of the sojourn times in asymptomatic ($1/\alpha$) and symptomatic ($1/\kappa$) compartments. In line with [7], it is assumed that the mean exposed and quarantined periods are the same ($1/\alpha$) and the mean infectious and hospitalized periods are the same ($1/\kappa$).

Table 1
Description of variables and parameters of the model (6).

Variable	Description
$S(t)$	Population of susceptible individuals
$E_i(t)$	Population of exposed individuals in ith exposed stage ($i = 1,\ldots,m$)
$I_j(t)$	Population of infected individuals in jth infectious stage ($j = 1,\ldots,n$)
$Q_i(t)$	Population of quarantined individuals in ith quarantined stage ($i = 1,\ldots,m$)
$H_j(t)$	Population of hospitalized individuals in jth hospitalized stage ($j = 1,\ldots,n$)
$R(t)$	Population of recovered individuals
Parameter	Description
Π	Recruitment rate
β	Effective contact rate
$d_j\kappa$	Progression rate from infectious stage j to stage $j + 1$ ($j = 1,\ldots,n$)
$c_j\kappa$	Progression rate from hospitalized stage j to stage $j + 1$ ($j = 1,\ldots,n$)
σ_i	Quarantine rate of exposed individuals in stage i
$a_i\alpha$	Progression rate from exposed stage i to stage $i + 1$ ($i = 1,\ldots,m - 1$)
$a_m\alpha$	Progression rate of exposed individuals in stage m to first infectious stage
$b_i\alpha$	Progression rate from quarantined stage i to stage $i + 1$ ($i = 1,\ldots,m - 1$)
$b_m\alpha$	Hospitalization rate of quarantined individuals in stage m
ϕ_j	Hospitalization rate of infectious individuals in jth infectious stage ($j = 1,\ldots,n$)
ψ	Rate of loss of infection-acquired immunity
γ_1	Recovery rate of infectious individuals in stage n
γ_2	Recovery rate of hospitalized individuals in stage n
δ_j $(1 \leqslant j \leqslant n)$	Disease-induced death rate of individuals in jth infectious stage
δ_j $(n + 1 \leqslant j \leqslant 2n)$	Disease-induced death rate of individuals in $(n - j)$th hospitalized stage
μ	Natural death rate

Let,

$$E = \sum_{i=1}^{m} \frac{a_i E_i}{m}, \quad I = \sum_{j=1}^{n} \frac{d_j I_j}{n}, \quad Q = \sum_{i=1}^{m} \frac{b_i Q_i}{m} \quad \text{and} \quad H = \sum_{j=1}^{n} \frac{c_j H_j}{n}. \tag{4}$$

It follows from (2) and (4), using the properties of gamma distribution ([12]; see also Appendix A for a brief description), that the compartments E, I, Q and H indeed have gamma distributions, given, respectively, by

$$\begin{aligned} p_E(s) &= \tfrac{(m\alpha)^m e^{-m\alpha s} s^{m-1}}{\Gamma(m)}; \quad m \geqslant 1, \\ p_I(s) &= \tfrac{(n\kappa)^n e^{-n\kappa s} s^{n-1}}{\Gamma(n)}; \quad n \geqslant 1, \\ p_Q(s) &= \tfrac{(m\alpha)^m e^{-m\alpha s} s^{m-1}}{\Gamma(m)}; \quad m \geqslant 1, \\ p_H(s) &= \tfrac{(n\kappa)^n e^{-n\kappa s} s^{n-1}}{\Gamma(n)}; \quad n \geqslant 1, \end{aligned}$$

where the associated exposed, infectious, quarantined and hospitalized periods are given, respectively, by (see also [7,33])

$$\begin{aligned} T_E &= \tfrac{1}{\alpha}, \\ T_I &= \tfrac{1}{\kappa}, \\ T_Q &= \tfrac{1}{\alpha}, \\ T_H &= \tfrac{1}{\kappa}. \end{aligned}$$

The above formulation ((3) and (4)) reduces to that in [7] by setting $a_i = b_i = m$ (for $i = 1,\ldots,m$) and $c_j = d_j = n$ (for $j = 1,\ldots,n$). In other words, it should be emphasized that the main distinction between the formulation in the current study and that in [7] is that, here, it is assumed that the sojourn periods in each of the four compartments, E, I, Q, and H, given by $1/\alpha$, $1/\kappa$, $1/\alpha$ and $1/\kappa$, respectively, are distributed (not necessarily equally) among the various sub stages (whereas, these periods are distributed equally at each related stage in [7]). Eichner et al. [6] considered 9 latent and 19 infectious stages to model the transmission dynamics of pandemic influenza.

It is worth stating that although the sums defined in (4) are gamma distributed, the actual (true) total number of infected individuals, E_{true}, I_{true}, Q_{true} and H_{true}, given, respectively, by

$$E_{\text{true}} = \sum_{i=1}^{m} E_i, \quad I_{\text{true}} = \sum_{j=1}^{n} I_j, \quad Q_{\text{true}} = \sum_{i=1}^{m} Q_i \quad \text{and} \quad H_{\text{true}} = \sum_{j=1}^{n} H_j, \tag{5}$$

are not necessarily gamma distributed. However, the different sums in (4) have the same means, with their respective sums given in (5), but different variances.

Thus, putting all these formulations and assumptions together, it follows that the model for the transmission dynamics of an infectious disease in the presence of exposed, quarantine, infectious and isolation periods, subject to gamma distributed sojourn periods, is given by the following non-linear system of differential equations (a flow diagram of the model is given in Fig. 1; and the associated variables and parameters are described in Table 1):

$$
\begin{aligned}
\frac{dS}{dt} &= \Pi + \psi R - \lambda S - \mu S,\\
\frac{dE_1}{dt} &= \lambda S - (\sigma_1 + a_1\alpha + \mu)E_1,\\
\frac{dE_2}{dt} &= a_1\alpha E_1 - (\sigma_2 + a_2\alpha + \mu)E_2,\\
\frac{dE_j}{dt} &= a_{j-1}\alpha E_{j-1} - (\sigma_j + a_j\alpha + \mu)E_j; \quad j = 3,\ldots,m,\\
\frac{dI_1}{dt} &= a_m\alpha E_m - (\phi_1 + d_1\kappa + \mu + \delta_1)I_1,\\
\frac{dI_2}{dt} &= d_1\kappa I_1 - (\phi_2 + d_2\kappa + \mu + \delta_2)I_2,\\
\frac{dI_j}{dt} &= d_{j-1}\kappa I_{j-1} - (\phi_j + d_j\kappa + \mu + \delta_j)I_j; \quad j = 3,\ldots,n-1,\\
\frac{dI_n}{dt} &= d_{n-1}\kappa I_{n-1} - (\phi_n + d_n\kappa + \mu + \delta_n)I_n,\\
\frac{dQ_1}{dt} &= \sigma_1 E_1 - (b_1\alpha + \mu)Q_1,\\
\frac{dQ_2}{dt} &= \sigma_2 E_2 + b_1\alpha Q_1 - (b_2\alpha + \mu)Q_2,\\
\frac{dQ_j}{dt} &= \sigma_j E_j + b_{j-1}\alpha Q_{j-1} - (b_j\alpha + \mu)Q_j; \quad j = 3,\ldots,m,\\
\frac{dH_1}{dt} &= b_m\alpha Q_m + \phi_1 I_1 - (c_1\kappa + \mu + \delta_{n+1})H_1,\\
\frac{dH_2}{dt} &= \phi_2 I_2 + c_1\kappa H_1 - (c_2\kappa + \mu + \delta_{n+2})H_2,\\
\frac{dH_j}{dt} &= \phi_j I_j + c_{j-1}\kappa H_{j-1} - (c_j\kappa + \mu + \delta_{n+j})H_j; \quad j = 3,\ldots,n-1,\\
\frac{dH_n}{dt} &= \phi_n I_n + c_{n-1}\kappa H_{n-1} - (c_n\kappa + \mu + \delta_{2n})H_n,\\
\frac{dR}{dt} &= \gamma_1 I_n + \gamma_2 H_n - (\psi + \mu)R.
\end{aligned} \tag{6}
$$

The model (6) extends the multi-stage model given in [7] by

(i) including a term for the loss of infection-acquired immunity (at the rate ψ). Although the numerical simulations to be carried out in this study are largely based on the 2003 SARS outbreaks (which was a single season epidemic), the model (6) is robust enough to enable the assessment of the transmission dynamics of any arbitrary disease where the infection-acquired immunity is lost either during a single season or in multiple seasons (such as the case of influenza, malaria, and some childhood diseases);
(ii) including disease-induced death (at rates δ_i; $i = 1,2,\ldots,2n$). Most diseases, such as HIV, malaria, influenza, TB, etc., have significant disease-induced mortality. Hence, it is crucial that this feature be incorporated in modeling studies;
(iii) assuming the average sojourn periods in the exposed, quarantined, infectious and hospitalized classes are distributed (not necessarily equally) among the various stages (these periods are assumed to be equally distributed among each of the aforementioned four infected compartments in [7]). Although, to our knowledge, there is no definitive epidemiological data to suggest that these periods are equally or unequally distributed, the model (6) is general enough to allow for the assessment of each of the two cases;
(iv) assuming varied rates of quarantine and isolation in each quarantine and isolation stage (same rates are used in [7] in all quarantine and isolation stages). This assumption allows for the assessment of progressive refinement of quarantine and isolation measures (this was evident during 2003 SARS outbreaks [8,17]).

The model (6) is denoted by GD1 for comparison purposes. It is worth emphasizing that the model (6) reduces to the model in [7] by setting $\psi = \delta_1 = \delta_2 = \cdots = \delta_{2n} = 0$, $a_1 = a_2 = \cdots = a_m = b_1 = b_2 = \cdots = b_m = m$, $c_1 = c_2 = \cdots = c_n = d_1 = d_2 = \cdots = d_n = n$, $\phi_1 = \cdots = \phi_n = \phi$ and $\sigma_1 = \cdots = \sigma$. Also, the model (6) is an extension of the model given in [24] by considering m stages for the exposed (E_i; $i = 1,2,\ldots,m$) and quarantined (Q_i; $i = 1,2,\ldots,m$) individuals and n stages for the infectious (I_j; $j = 1,2,\ldots,n$) and the hospitalized (H_j; $j = 1,2,\ldots,n$) individuals (i.e., the model (6) reduces to the model in [24] by setting $n = m = 1$, taking into account the assumption that hospitalized individuals do not transmit infection; this assumption is relaxed in [24]).

In addition to formulating the model in terms of gamma-distributed waiting times for the associated disease stages, this study contributes by way of carrying out a detailed rigorous mathematical analysis of the model (6). In particular, global asymptotic stability results for the equilibria of the model will be proven (under certain conditions). Furthermore, the model (6) is used to evaluate the impact of the use of quarantine and isolation in combatting the spread of a given communicable disease (such as SARS). This study offers not only important extensions to the model presented in [7], it also contributes by extending some of the mathematical results presented in [7] (particularly global stability proof of the associated endemic equilibrium of the extended model (6)).

2.1. Basic properties

Since the model (6) monitors human populations, all its associated parameters are non-negative. Further, the following basic results can be easily established (see, for instance, [24,27]):

Theorem 1. *The state variables of the model (6) are non-negative for all time. In other words, solutions of the model system (6) with positive initial data will remain positive for all time $t > 0$.*

Lemma 1. *The closed set*

$$\mathcal{D} = \left\{ (S, E_1, \ldots, E_m, I_1, \ldots, I_n, Q_1, \ldots, Q_m, H_1, \ldots, H_n, R) \in \mathbb{R}_+^{2(m+n+1)} : S + \sum_{i=1}^{m} E_i + Q_i + \sum_{j=1}^{n} I_j + H_j + R \leqslant \frac{\Pi}{\mu} \right\}$$

is positively-invariant. (7)

3. Local stability of disease-free equilibrium (DFE)

The model (6) has a DFE, obtained by setting the right-hand sides of the equations to zero, given by is given by

$$\Omega_0 = (S^*, E_1^*, \ldots, E_m^*, I_1^*, \ldots, I_n^*, Q_1^*, \ldots, Q_m^*, H_1^*, \ldots, H_n^*, R^*) = (\Pi/\mu, 0, \ldots, 0). \tag{8}$$

The next generation operator method [4,28] will be used to explore the local stability of Ω_0. Using the notation in [28], the non-negative matrix, F, of the new infection terms, and the M-matrix, V, of the transition terms associated with the model (6), are given, respectively, by

$$F = \begin{pmatrix} A_F & B_F & C_F \end{pmatrix},$$

and,

$$V = \begin{pmatrix} A_V & B_V \\ C_V & D_V \end{pmatrix},$$

where, A_F is $2(m+n) \times m$ zero matrix, C_F, B_V are $2(m+n) \times (m+n)$, $(m+n) \times (m+n)$ zero matrices, respectively. Furthermore, B_F is a $2(m+n) \times n$ matrix, given by

$$B_F = \begin{pmatrix} \beta & \beta & \cdots & \beta \\ 0 & 0 & \cdots & 0 \\ \vdots & \vdots & & \vdots \\ 0 & 0 & \cdots & 0 \end{pmatrix}.$$

The matrices, A_V, C_V and D_V are $(m+n) \times (m+n)$ are given by

$$A_V = \begin{pmatrix} k_1 & & & & & & & & \\ -a_1\alpha & k_2 & & & & & & & \\ & -a_2\alpha & k_3 & & & & & & \\ & & \ddots & \ddots & & & & & \\ & & & -a_m\alpha & k_{m+1} & & & & \\ & & & & -d_1\kappa & k_{m+2} & & & \\ & & & & & -d_2\kappa & k_{m+3} & & \\ & & & & & & \ddots & \ddots & \\ & & & & & & & -d_{n-1}\kappa & k_{m+n} \end{pmatrix},$$

$$C_V = \begin{pmatrix} -\sigma_1 &&&&&&& \\ & -\sigma_2 &&&&&& \\ && \ddots &&&&& \\ &&& -\sigma_m &&&& \\ &&&& -\phi_1 &&& \\ &&&&& -\phi_2 && \\ &&&&&& \ddots & \\ &&&&&&& -\phi_n \end{pmatrix},$$

and,

$$D_V = \begin{pmatrix} k_{m+n+1} &&&&&&& \\ -b_1\alpha & k_{m+n+2} &&&&&& \\ & -b_2\alpha & k_{m+n+3} &&&&& \\ && \ddots & \ddots &&&& \\ &&& -b_m\alpha & k_{2m+n+1} &&& \\ &&&& -c_1\kappa & k_{2m+n+2} && \\ &&&&& -c_2\kappa & k_{2m+n+3} & \\ &&&&&& \ddots & \ddots \\ &&&&&&& -c_{n-1}\kappa \quad k_{2(m+n)} \end{pmatrix},$$

with,

$$k_j = \begin{cases} \sigma_j + a_j\alpha + \mu; & 1 \leqslant j \leqslant m; \\ \phi_{j-m} + d_{j-m}\kappa + \mu + \delta_{j-m}; & m+1 \leqslant j \leqslant m+n; \\ b_{j-(m+n)}\alpha + \mu; & n+m+1 \leqslant j \leqslant 2m+n; \\ c_{j-(2m+n)}\kappa + \mu + \delta_{j-2m}; & 2m+n+1 \leqslant j \leqslant 2(m+n). \end{cases}$$

Let,

$$\begin{aligned} A_l &= \alpha^{m-l+1}\prod_{i=l}^{m} a_i, \quad l = 1,2,\ldots,m; \\ B_l &= \prod_{i=l}^{m+n-1} k_i, \quad l = 1,2,\ldots,m+n-1;\ B_{m+n} = 1; \\ D_l &= \frac{A_l}{B_l}; \quad l = 1,2,\ldots,m;\ D_{m+1} = \frac{1}{B_{m+1}}; \\ C_{p,q} &= \kappa^{p-1}\prod_{i=1}^{p-1} d_{i+q-1} + \prod_{s=2}^{p} k_{m+s+q-1} + \sum_{t=1}^{p-2}\kappa^t \prod_{i=1}^{t} d_{i+q-1} \prod_{s=2+t}^{p} k_{m+s+q-1};\ p = 3,\ldots,n,\ q = n+1-p; \\ C_{1,n} &= 1 \quad \text{and} \quad C_{2,n-1} = \kappa d_{n-1} + k_{m+n}. \end{aligned} \tag{9}$$

It follows that the *control reproduction number* [1,10], denoted by $\mathcal{R}_c = \rho(FV^{-1})$, where ρ is the spectral radius, is given by

$$\mathcal{R}_c = \frac{\beta D_1 C_{n,1}}{k_{m+n}}.$$

Using Theorem 2 in [28], the following result is established.

Lemma 2. *The DFE of the model* (6), *given by* (8), *is locally-asymptotically stable* (*LAS*) *if* $\mathcal{R}_c < 1$, *and unstable if* $\mathcal{R}_c > 1$.

The epidemiological implication of Lemma 2 is that the disease can be eliminated from the community (when $\mathcal{R}_c < 1$) if the initial sizes of the sub-populations of the model are in the basin of attraction of the DFE (Ω_0). For disease elimination to be independent of the initial sizes of sub-populations, the global asymptotic stability of the DFE must be established for $\mathcal{R}_c < 1$.

3.1. Global stability of DFE

Theorem 2. *The DFE of the model* (6), *given by* (8), *is globally-asymptotically stable* (*GAS*) *in* $\mathcal{D}$ *whenever* $\mathcal{R}_c \leqslant 1$.

Proof. Consider the following Lyapunov function (with the coefficients B, C and D as defined in (9)):

$$\mathcal{F} = \left(\frac{k_{m+n}\mathcal{R}_c}{\beta}\right)E_1 + C_{n,1}D_2E_2 + \sum_{j=3}^{m} C_{n,1}D_jE_j + \sum_{j=1}^{n-1}\left(\frac{C_{n-j+1,j}}{B_{m+j}}\right)I_j + I_n$$

with Lyapunov derivative (where a dot represents differentiation with respect to time) given by

$$\begin{aligned}
\dot{\mathcal{F}} &= \left(\frac{k_{m+n}\mathcal{R}_c}{\beta}\right)\dot{E}_1 + C_{n,1}D_2\dot{E}_2 + \sum_{j=3}^{m} C_{n,1}D_j\dot{E}_j + \sum_{j=1}^{n-1}\left(\frac{C_{n-j+1,j}}{B_{m+j}}\right)\dot{I}_j + \dot{I}_n \\
&= \left(\frac{k_{m+n}\mathcal{R}_c}{\beta}\right)\left(\frac{\beta S\sum_{j=1}^{n} I_j}{N} - k_1E_1\right) + C_{n,1}D_2(a_1\alpha E_1 - k_2E_2) \\
&\quad + \sum_{j=3}^{m-1} C_{n,1}D_j(a_{j-1}\alpha E_{j-1} - k_jE_j) + C_{n,1}D_m(a_{m-1}\alpha E_{m-1} - k_mE_m) \\
&\quad + \frac{C_{n,1}}{B_{m+1}}(a_m\alpha E_m - k_{m+1}I_1) + \sum_{j=2}^{n-1}\frac{C_{n-j+1,j}}{B_{m+j}}(d_{j-1}\kappa I_{j-1} - k_{m+j}I_j) + d_{n-1}\kappa I_{n-1} - k_{m+n}I_n \\
&\leqslant k_{m+n}\mathcal{R}_c\sum_{j=1}^{n} I_j - \left(\frac{k_1k_{m+n}\mathcal{R}_c}{\beta}\right)E_1 + C_{n,1}D_2(a_1\alpha E_1 - k_2E_2) \\
&\quad + \sum_{j=3}^{m-1} C_{n,1}D_j(a_{j-1}\alpha E_{j-1} - k_jE_j) + C_{n,1}D_m(a_{m-1}\alpha E_{m-1} - k_mE_m) \\
&\quad + \frac{C_{n,1}}{B_{m+1}}(a_m\alpha E_m - k_{m+1}I_1) + \sum_{j=2}^{n-1}\frac{C_{n-j+1,j}}{B_{m+j}}(d_{j-1}\kappa I_{j-1} - k_{m+j}I_j) \\
&\quad + d_{n-1}\kappa I_{n-1} - k_{m+n}I_n, \quad \text{since } S \leqslant N \text{ in } \mathcal{D}, \\
&= k_{m+n}\mathcal{R}_c\sum_{j=1}^{n} I_j + \left(-\frac{k_1k_{m+n}\mathcal{R}_c}{\beta} + C_{n,1}D_2a_1\alpha\right)E_1 + \sum_{j=3}^{m+1} C_{n,1}D_ja_{j-1}\alpha E_{j-1} \\
&\quad - \sum_{j=2}^{m} C_{n,1}D_jk_jE_j + \sum_{j=2}^{n}\frac{C_{n-j+1,j}}{B_{m+j}}d_{j-1}\kappa I_{j-1} - \sum_{j=1}^{n-1}\frac{C_{n-j+1,j}}{B_{m+j}}k_{m+j}I_j - k_{m+n}I_n, \\
&= k_{m+n}\mathcal{R}_c\sum_{j=1}^{n} I_j + \sum_{j=2}^{m} C_{n,1}(D_{j+1}a_j\alpha - D_jk_j)E_j + \sum_{j=1}^{n-1}\left(\frac{d_j\kappa C_{n-j,j+1}}{B_{m+j+1}} - \frac{k_{m+j}C_{n-j+1,j}}{B_{m+j}}\right)I_j - k_{m+n}I_n.
\end{aligned}$$

It can be shown, after some lengthy algebraic manipulations, that

$$D_{j+1}a_j\alpha - D_jk_j = 0,$$

and,

$$\frac{d_j\kappa C_{n-j,j+1}}{B_{m+j+1}} - \frac{k_{m+j}C_{n-j+1,j}}{B_{m+j}} = -k_{m+n}.$$

Hence,

$$\dot{\mathcal{F}} \leqslant k_{m+n}(\mathcal{R}_c - 1)\sum_{j=1}^{n} I_j \leqslant 0 \quad \text{for } \mathcal{R}_c \leqslant 1.$$

Since all the parameters of the model (6) and variables are non-negative, it follows that $\dot{\mathcal{F}} \leqslant 0$ for $\mathcal{R}_c \leqslant 1$ with $\dot{\mathcal{F}} = 0$ if and only if $I_1 = I_2 = \cdots = I_n = 0$. Hence, $\mathcal{F}$ is a Lyapunov function on $\mathcal{D}$. Therefore, by the LaSalle's Invariance Principle [9],

$$\begin{aligned}
&\lim_{t\to\infty} E_i(t) = 0, \quad \text{for all } i = 1,\ldots,m; \\
&\lim_{t\to\infty} I_j(t) = 0, \quad \text{for all } j = 1,\ldots,n.
\end{aligned} \tag{10}$$

It is clear from (10) that $\limsup_{t\to\infty} E_1 = 0$. Thus, for sufficiently small $\varpi_1 > 0$, there exists a constant $N_1 > 0$ such that $\limsup_{t\to\infty} E_1 \leqslant \varpi_1$ for all $t > N_1$. It follows from the $(m + n + 2)$th equation of the model (6) that, for $t > N_1$,

$$\dot{Q}_1 \leqslant \sigma_1\varpi_1 - k_{m+n+1}Q_1.$$

Thus, by comparison theorem [26],

$$Q_1^{\infty} = \limsup_{t\to\infty} Q_1 \leqslant \frac{\sigma_1\varpi_1}{k_{m+n+1}},$$

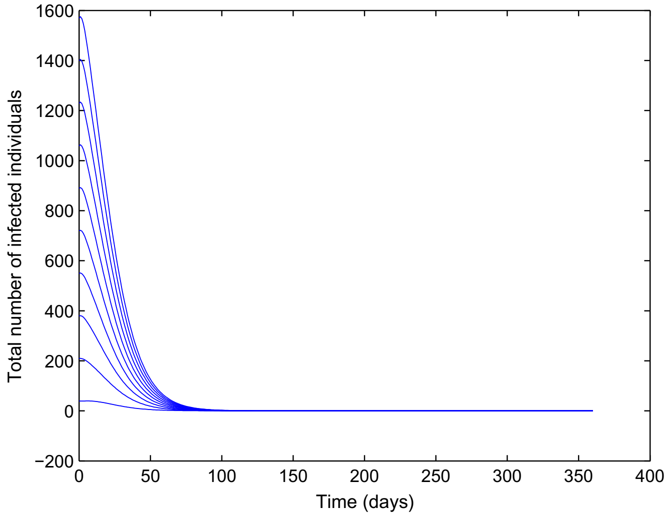

Fig. 2. Simulation of the model (6) showing the total number of infected individuals as a function of time for $\mathcal{R}_c < 1$. Parameter values used are as in Tables 2 and 4 with $\beta = 0.2$, $m = 2$, $n = 3$, $a_1 = b_1 = 1.5$, $a_2 = b_2 = 3$, $c_1 = d_1 = c_2 = d_2 = c_3 = d_3 = 3$ (so that, $\mathcal{R}_c = 0.4610$).

Table 2
Estimated values of the parameters of the model (6).

Parameters	Values (per day)	Sources
β	[0.1,0.5]	[8,21]
μ	0.0000351	[13]
κ	0.042553	[2]
δ_i; $i = 1,\ldots,n$	0.04227	[17]
δ_i; $i = n+1,\ldots,2n$	0.027855	[2]
α	0.156986	[5]
ϕ_n	0.20619	[2]
Π	136	[8]
σ_m	0.1	[8]
ψ	0.005	Assumed

so that, by letting $\varpi_1 \to 0$,

$$Q_1^{\infty} = \limsup_{t\to\infty} Q_1 \leqslant 0. \quad (11)$$

Similarly (by using $\lim\inf_{t\to\infty} E_1 = 0$), it can be shown that

$$Q_{1_\infty} = \liminf_{t\to\infty} Q_1 \geqslant 0. \quad (12)$$

Thus, it follows from (11) and (12) that

$$Q_{1_\infty} \geqslant 0 \geqslant Q_1^{\infty}.$$

Hence,

$$\lim_{t\to\infty} Q_1 = 0. \quad (13)$$

Similarly, it can be shown that

$$\begin{aligned}
&\lim_{t\to\infty} Q_i(t) = 0, \quad \text{for all } i = 2,\ldots,m,\\
&\lim_{t\to\infty} H_j(t) = 0, \quad \text{for all } j = 1,\ldots,n,\\
&\lim_{t\to\infty} R(t) = 0, \quad \lim_{t\to\infty} S(t) = \Pi/\mu.
\end{aligned} \quad (14)$$

Thus, by combining (10), (13) and (14), it follows that every solution of the equations in the model (6), with initial conditions in $\mathcal{D}$, approaches the DFE, Ω_0, as $t \to \infty$ when $\mathcal{R}_c \leqslant 1$. $\square$

Table 3
Values of a_i, b_i, c_i and d_i ($i = 1,2,3$) for various number of disease stages (m and n).

Number of stages	Values of a_i, b_i, c_i, d_i
$m = n = 1$	$a_1 = b_1 = 1$, $c_1 = d_1 = 1$
$m = n = 2$	$a_1 = b_1 = 1.5$, $a_2 = b_2 = 3$, $c_1 = d_1 = 1.5$, $c_2 = d_2 = 3$
$m = n = 3$	$a_1 = b_1 = 2$, $a_2 = b_2 = 3$, $a_3 = b_3 = 6$, $c_1 = d_1 = 2$, $c_2 = d_2 = 3$, $c_3 = d_3 = 6$

Table 4
Quarantine and hospitalization rates for various number of disease stages (m and n).

Number of stages	Quarantine rates	Hospitalization rates
$m = n = 1$	$\sigma_1 = 0.1$	$\phi_1 = 0.20619$
$m = n = 2$	$\sigma_1 = 0.05$, $\sigma_2 = 0.1$	$\phi_1 = 0.1$, $\phi_2 = 0.20619$
$m = n = 3$	$\sigma_1 = 0.03333$, $\sigma_2 = 0.05$, $\sigma_3 = 0.1$	$\phi_1 = 0.0666$, $\phi_2 = 0.1$, $\phi_3 = 0.20619$

Theorem 2 shows that if the use of quarantine and isolation can bring (and keep) the threshold quantity, $\mathcal{R}_c$, to a value less than unity, then the disease will be eliminated from the community (i.e., the condition $\mathcal{R}_c < 1$ is necessary and sufficient for disease elimination). Fig. 2 depicts numerical results obtained by simulating the model (6), with $m = 2$ and $n = 3$, using various initial conditions for the case $\mathcal{R}_c < 1$. All solutions converged to the DFE, Ω_0, (in line with Theorem 2). It should be mentioned that, unless otherwise stated, simulations of the model (6) are carried out using the parameter values in Tables 2 and 4. These parameter values are consistent with those associated with the 2003 SARS outbreaks [2,5,8,17]. It is worth mentioning that the progressive refinement of quarantine and isolation measures is incorporated in all numerical simulations in this study (unless otherwise stated) by using smaller values of σ_1 and σ_2, in comparison to σ_3; and also smaller values of ϕ_1 and ϕ_2, in relation to ϕ_3 (see Table 4).

4. Existence and stability of endemic equilibria

In this section, the possible existence and stability of endemic (positive) equilibria of the model (6) (i.e., equilibria where at least one of the infected components of the model is non-zero) will be explored.

4.1. Existence of endemic equilibrium point (EEP)

Define

$$\Omega_1 = (S^{**}, E_1^{**}, E_2^{**}, \ldots, E_m^{**}, I_1^{**}, I_2^{**}, \cdots, I_n^{**}, Q_1^{**}, Q_2^{**}, \ldots, Q_m^{**}, H_1^{**}, H_2^{**}, \cdots, H_n^{**}, R^{**})$$

to be any arbitrary endemic equilibrium of the model (6). Solving the equations of the model at endemic steady-state gives

$$\begin{aligned}
&S^{**} = \frac{\Pi + \psi R^{**}}{\lambda^{**} + \mu}, \quad E_1^{**} = \frac{\lambda^{**} S^{**}}{k_1}, \quad E_j^{**} = \frac{a_{j-1}\alpha E_{j-1}^{**}}{k_j} \quad \text{for } j = 2, \ldots, m,\\
&I_1^{**} = \frac{a_m \alpha E_m^{**}}{k_{m+1}}, \quad I_2^{**} = \frac{d_1 \kappa I_1^{**}}{k_{m+2}}, \quad I_j^{**} = \frac{d_{j-1}\kappa I_{j-1}^{**}}{k_{m+j}} \quad \text{for } j = 3, \ldots, n,\\
&Q_1^{**} = \frac{\sigma_1 E_1^{**}}{k_{m+n+1}}, \quad Q_j^{**} = \frac{\sigma_j E_j^{**} + b_{j-1}\alpha Q_{j-1}^{**}}{k_{m+n+j}} \quad \text{for } j = 2, \ldots, m,\\
&H_1^{**} = \frac{\phi_1 I_1^{**} + b_n \alpha Q_n^{**}}{k_{2m+n+1}}, \quad H_j^{**} = \frac{\phi_j I_j^{**} + c_{j-1}\kappa H_{j-1}^{**}}{k_{2m+n+j}} \quad \text{for } j = 2, \ldots, n,\\
&R^{**} = \frac{\gamma_1 I_n^{**} + \gamma_2 H_n^{**}}{\psi + \mu}.
\end{aligned} \tag{15}$$

The force of infection λ, given by (1), can be expressed at endemic steady-state as

$$\lambda^{**} = \frac{\beta \sum_{j=1}^{n} I_j^{**}}{N^{**}}. \tag{16}$$

As in [24], the expressions in (15) are re-written in terms of $\lambda^{**}S^{**}$, for computational convenience, as below:

$$
\begin{aligned}
&E_1^{**}=\frac{\lambda^{**}S^{**}}{k_1},\quad E_j^{**}=\left(\frac{\alpha^{j-1}}{k_1}\prod_{l=2}^{j}\frac{a_{l-1}}{k_l}\right)\lambda^{**}S^{**}\quad \text{for } j=2,\dots,m,\\
&I_1^{**}=\left(\frac{\alpha^{m}}{k_1}\prod_{l=2}^{m+1}\frac{a_{l-1}}{k_l}\right)\lambda^{**}S^{**},\quad I_j^{**}=\left(\frac{\alpha^{m}\kappa^{j-1}}{k_1}\prod_{l=2}^{m+1}\frac{a_{l-1}}{k_l}\prod_{l=2}^{j}\frac{d_{l-1}}{k_{m+j}}\right)\lambda^{**}S^{**}\quad \text{for } j=2,\dots,n,\\
&Q_1^{**}=\frac{\sigma_1\lambda^{**}S^{**}}{k_1k_{m+n+1}}=p_1\lambda^{**}S^{**},\quad Q_j^{**}=p_j\lambda^{**}S^{**}\quad \text{for } j=2,\dots,m,\\
&H_1^{**}=\left(\frac{\alpha^{m}\phi_1}{k_1k_{2m+n+1}}\prod_{l=2}^{m+1}\frac{a_{l-1}}{k_l}+\frac{b_m\alpha p_m}{k_{2m+n+1}}\right)\lambda^{**}S^{**}=q_1\lambda^{**}S^{**},\quad H_j^{**}=q_j\lambda^{**}S^{**}\quad \text{for } j=2,\dots,n,\\
&R^{**}=\left(\frac{\alpha^{m}\kappa^{n-1}\gamma_1}{k_1(\psi+\mu)}\prod_{l=2}^{m+1}\frac{a_{l-1}}{k_l}\prod_{l=2}^{n}\frac{d_{l-1}}{k_{m+n}}+\frac{q_n\gamma_2}{\psi+\mu}\right)\lambda^{**}S^{**},
\end{aligned}
\tag{17}
$$

where,

$$
\begin{aligned}
&p_1=\frac{\sigma_1}{k_1k_{m+n+1}},\quad q_1=\frac{\alpha^{m}\phi_1}{k_1k_{2m+n+1}}\prod_{l=2}^{m+1}\frac{a_{l-1}}{k_l}+\frac{b_m\alpha p_m}{k_{2m+n+1}},\\
&p_j=\frac{b_{j-1}\alpha p_{j-1}}{k_{m+n+j}}+\frac{\sigma_i\alpha^{j-1}}{k_{m+n+j}k_1}\prod_{l=2}^{j}\frac{a_{l-1}}{k_l}\ \text{ for } j=2,\dots,m,
\end{aligned}
$$

and,

$$
q_j=\frac{c_{j-1}\kappa q_{j-1}}{k_{2m+n+j}}+\frac{\phi_j\alpha^{m}\kappa^{j-1}}{k_1k_{2m+n+j}}\prod_{l=2}^{m+1}\frac{a_{l-1}}{k_l}\prod_{l=2}^{j}\frac{d_{l-1}}{k_{m+j}}\quad \text{for } j=2,\dots,n.
$$

Substituting the expressions in (17) into (16) gives

$$
\begin{aligned}
&\lambda^{**}S^{**}+\frac{\lambda^{**}S^{**}\lambda^{**}}{k_1}+\sum_{i=2}^{m}\left(\frac{\alpha^{j-1}}{k_1}\prod_{l=2}^{j}\frac{a_{l-1}}{k_l}\right)\lambda^{**}S^{**}\lambda^{**}+\left(\frac{\alpha^{m}}{k_1}\prod_{l=2}^{m+1}\frac{a_{l-1}}{k_l}\right)\lambda^{**}S^{**}\lambda^{**}\\
&\quad+\sum_{j=2}^{n}\left(\frac{\alpha^{m}\kappa^{j-1}}{k_1}\prod_{l=2}^{m+1}\frac{a_{l-1}}{k_l}\prod_{l=2}^{j}\frac{d_{l-1}}{k_{m+j}}\right)\lambda^{**}S^{**}\lambda^{**}+\sum_{i=1}^{m}q_i\lambda^{**}S^{**}\lambda^{**}+\sum_{j=1}^{n}p_j\lambda^{**}S^{**}\lambda^{**}\\
&\quad+\left(\frac{\alpha^{m}\kappa^{n-1}\gamma_1}{k_1(\psi+\mu)}\prod_{l=2}^{m+1}\frac{a_{l-1}}{k_l}\prod_{l=2}^{n}\frac{d_{l-1}}{k_{m+n}}+\frac{q_n\gamma_2}{\psi+\mu}\right)\lambda^{**}S^{**}\lambda^{**}\\
&\quad=\beta\left[\frac{\alpha^{m}}{k_1}\prod_{l=2}^{m+1}\frac{a_{l-1}}{k_l}+\sum_{j=2}^{n}\left(\frac{\alpha^{m}\kappa^{j-1}}{k_1}\prod_{l=2}^{m+1}\frac{a_{l-1}}{k_l}\prod_{l=2}^{j}\frac{d_{l-1}}{k_{m+j}}\right)\right]\lambda^{**}S^{**}.
\end{aligned}
\tag{18}
$$

Dividing each term in (18) by $\lambda^{**}S^{**}$ (and noting that $\lambda^{**}S^{**}\neq 0$ at the endemic steady-state) gives

$$1+W\lambda^{**}=\mathcal{R}_c,$$

where,

$$
W=\frac{1}{k_1}+\sum_{i=2}^{m+1}\frac{\alpha^{j-1}}{k_1}\prod_{l=2}^{j}\frac{a_{l-1}}{k_l}+\sum_{j=2}^{n}\frac{\alpha^{m}\kappa^{j-1}}{k_1}\prod_{l=2}^{m+1}\frac{a_{l-1}}{k_l}\prod_{l=2}^{j}\frac{d_{l-1}}{k_{m+j}}+\sum_{i=1}^{m}q_i+\sum_{j=1}^{n}p_j+\frac{\alpha^{m}\kappa^{n-1}\gamma_1}{k_1(\psi+\mu)}\prod_{l=2}^{m+1}\frac{a_{l-1}}{k_l}\prod_{l=2}^{n}\frac{d_{l-1}}{k_{m+n}}+\frac{q_n\gamma_2}{\psi+\mu}\geqslant 0.
$$

Hence,

$$
\lambda^{**}=\frac{\mathcal{R}_c-1}{W}>0,\quad \text{whenever } \mathcal{R}_c>1.
\tag{19}
$$

The components of the unique endemic equilibrium Ω_1 can then be obtained by substituting the unique value of λ^{**}, given in (19), into the expressions in (17). This result is summarized below.

Lemma 3. *The model (6) has a unique endemic (positive) equilibrium, given by Ω_1, whenever $\mathcal{R}_c>1$.*

4.2. Global stability of endemic equilibrium for special case

Here, the global stability of the endemic equilibrium of the model (6) is given for the special case where the recovered individuals do not lose their infection-acquired immunity (i.e., $\psi = 0$) and the associated disease-induced mortality in all classes is negligible (so that, $\delta_1 = \delta_2 = \cdots \delta_{2n} = 0$). The model (6), with $\psi = \delta_1 = \delta_2 = \cdots = \delta_{2n} = 0$, then reduces to:

$$
\begin{aligned}
\frac{dS}{dt} &= \Pi - \lambda S - \mu S,\\
\frac{dE_1}{dt} &= \lambda S - f_1 E_1,\\
\frac{dE_2}{dt} &= a_1 \alpha E_1 - f_2 E_2,\\
\frac{dE_j}{dt} &= a_{j-1}\alpha E_{j-1} - f_j E_j;\ j = 3,\ldots,m,\\
\frac{dI_1}{dt} &= a_m \alpha E_m - f_{m+1} I_1,\\
\frac{dI_j}{dt} &= d_{j-1}\kappa I_{j-1} - f_{m+j} I_j;\ j = 2,\ldots,n,\\
\frac{dQ_1}{dt} &= \sigma_1 E_1 - f_{m+n+1} Q_1,\\
\frac{dQ_j}{dt} &= \sigma_j E_j + b_{j-1}\alpha Q_{j-1} - f_{m+n+j} Q_j;\ j = 2,\ldots,m,\\
\frac{dH_1}{dt} &= b_m \alpha Q_m + \phi_1 I_1 - f_{2m+n+1} H_1,\\
\frac{dH_j}{dt} &= \phi_j I_j + c_{j-1}\kappa H_{j-1} - f_{2m+n+j} H_j;\ j = 2,\ldots,n,\\
\frac{dR}{dt} &= \gamma_1 I_n + \gamma_2 H_n - \mu R.
\end{aligned}
\tag{20}
$$

Adding the equations of the reduced model (20) gives $dN/dt = \Pi - \mu N$. Hence, $N \to \Pi/\mu$ as $t \to \infty$. Thus, Π/μ is an upper bound of $N(t)$ provided that $N(0) \leqslant \Pi/\mu$. Further, if $N(0) > \Pi/\mu$, then $N(t)$ will decrease to this level. Using $N = \Pi/\mu$ in (1) gives a limiting (mass action) system given by (20) with

$$
\lambda = \beta_1 \sum_{j=1}^{n} I_j, \quad \text{where } \beta_1 = \frac{\beta\mu}{\Pi}. \tag{21}
$$

It can be shown that the associated reproduction number of the reduced model, (20) with (21), is given by

$$
\mathcal{R}_{cr} = \frac{\beta \widetilde{D_1}\, \widetilde{C_{n,1}}}{f_{m+n}},
$$

where,

$$
\widetilde{D_1} = \frac{\alpha^m \prod_{i=l}^{m} a_i}{\prod_{i=l}^{m+n-1} f_i} \quad \text{and} \quad \widetilde{C_{n,1}} = \kappa^{n-1} \prod_{i=1}^{p-1} d_i + \prod_{s=2}^{n} f_{m+s} + \sum_{t=1}^{n-2} \kappa^t \prod_{i=1}^{t} d_i \prod_{s=2+t}^{n} f_{m+s}.
$$

It is easy to show, using the technique in Section 4.1, that the reduced model, given by (20) with (21), has a unique EEP whenever $\mathcal{R}_{cr} > 1$.

Lemma 4. *The reduced model, given by (20) with (21), has a unique positive endemic equilibrium whenever $\mathcal{R}_{cr} > 1$.*

Furthermore, we claim the following result (see Appendix B for the proof).

Theorem 3. *The unique endemic equilibrium of the reduced model, given by (20) with (21), is GAS in $\mathcal{D} \setminus \mathcal{D}_0$ if $\mathcal{R}_{cr} > 1$.*

Simulations for the case when $\mathcal{R}_c > 1$ are depicted in Fig. 3, showing convergence of the solutions to the endemic equilibrium (in line with Theorem 3). Fig. 4 depicts the cumulative number of new infections as a function of quarantine rates, from which it is evident that the cumulative number of new infections decreases with increasing quarantine rate. Similar result is obtained by increasing the isolation rate (Fig. 5). It should be mentioned that the simulation results in Figs. 4 and 5 are consistent with those reported in [7]. Although the global asymptotic stability result given in Appendix B is for a special case (with $\psi = \delta_1 = \delta_2 = \cdots = \delta_{2n} = 0$), further extensive numerical simulations suggest that the endemic equilibrium Ω_1, of the full model (6), is GAS in $\mathcal{D} \setminus \mathcal{D}_0$ whenever $\mathcal{R}_c > 1$, suggesting the following conjecture.

Conjecture. *The unique endemic equilibrium of the model (6), denoted by Ω_1, is GAS in $\mathcal{D} \setminus \mathcal{D}_0$ if $\mathcal{R}_c > 1$.*

The effect of the number of disease stages for the exposed (m) and infectious (n) classes is monitored by simulating the model (6) with various values of $m = n$. The results obtained, depicted in Fig. 6, show an increase in the cumulative number of disease-related mortality with increasing values of $m = n$. Simulations for the cumulative number of probable SARS cases observed during the 2003 outbreaks in the Greater Toronto Area (GTA) of Canada are also carried out. The results obtained, for the case $m = n = 3$, are compared with those obtained using the exponentially-distributed (ED) equivalent of the model (6) (i.e., model (6) with $m = n = 1$) and another gamma-distributed version of the model (6) with $m = n = 3$, denoted by GD2, where the average sojourn time in each of the exposed, quarantined, hospitalized and infectious stages is shared equally

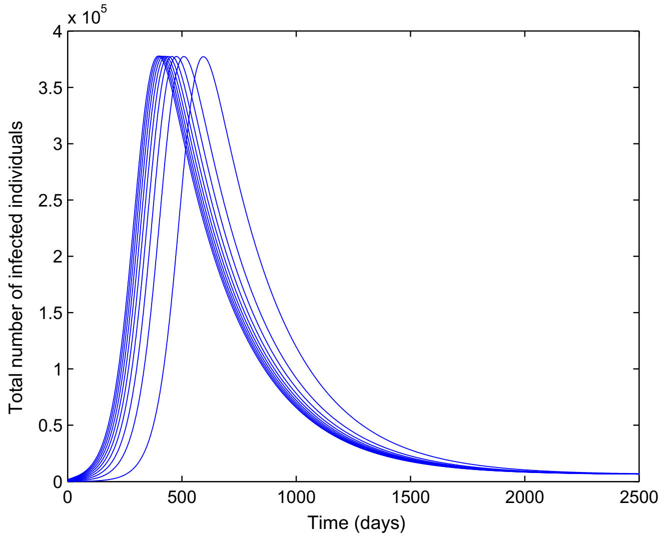

Fig. 3. Simulation of the model (6) showing the total number of infected individuals as a function of time for $\mathcal{R}_c > 1$. Parameter values used are as in Tables 2 and 4 with $\beta = 0.5$, $m = 2$, $n = 3$, $a_1 = b_1 = 1.5$, $a_2 = b_2 = 3$, $c_1 = d_1 = c_2 = d_2 = c_3 = d_3 = 3$ (so that, $\mathcal{R}_c = 1.1526$).

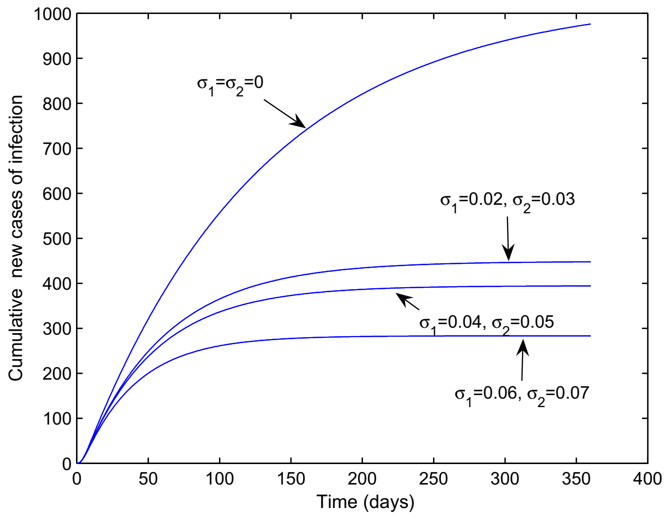

Fig. 4. Numerical simulations of the model (6) showing the cumulative number of new infections for various values of the quarantine parameters (σ_1 and σ_2). Parameter values used are as in Table 2, with $\beta = 0.15$, $m = 2$, $n = 3$, $a_1 = b_1 = 1.5$, $a_2 = b_2 = 3$, $c_1 = d_1 = c_2 = d_2 = c_3 = d_3 = 3$ and isolation rates as given in Table 4.

among each associated disease stage (this is similar to the model given in [7]). It should be mentioned that, in such a setting, the standard ED model has the associated reproduction number given by $\mathcal{R}_c = 0.6506$. Similarly, the GD2 and GD1 models have $\mathcal{R}_c = 0.6962$ and $\mathcal{R}_c = 0.9858$, respectively. Furthermore, about 250 probable SARS cases were reported for the GTA (see Fig. 2 in [8]). The simulation results obtained, depicted in Fig. 7, show that while the ED and GD2 models underestimated the observed number of probable cases, the GD1 model (6) gave a very good estimate of the observed data. It should be mentioned that the GD2 model is also competitive if the quarantine and isolation rates are distributed (unequally) to incorporate their progressive refinement (as in the case of the model GD1).

Similar comparison are made for the cumulative number of cases recorded for the Hong Kong SARS outbreaks (approximately 1750 cases were recorded in Hong Kong [8]). Here, too, the GD1 model is more competitive (Fig. 8). For these simulations, the ED, GD1 and GD2 models have $\mathcal{R}_c$ given by 0.7345, 0.9710 and 0.7861, respectively. It should be emphasized, however, that the reason why the GD1 model gives different results, compared to the GD2 model (for instance), is that the values of σ_1 and σ_2, and also ϕ_1 and ϕ_2, used in the simulations of the GD1 model are different from the quarantine (σ) and isolation (ϕ) rates used in the simulations of the GD2 model. While the values $\sigma_1 = 0.0333$, $\sigma_2 = 0.05$, $\sigma_3 = 0.1$ and $\phi_1 = 0.0666$,

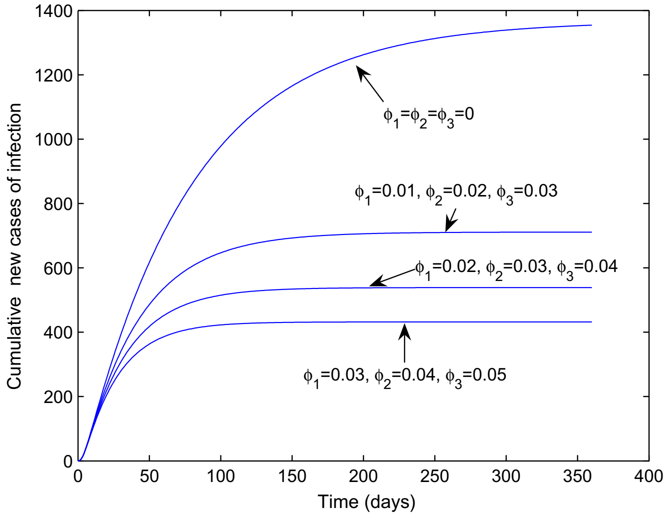

Fig. 5. Numerical simulations of the model (6) showing the cumulative number of new infections for various values of the isolation parameters (ϕ_1, ϕ_2 and ϕ_3). Parameter values used are as in Table 2, with $\beta = 0.15$, $m = 2$, $n = 3$, $a_1 = b_1 = 1.5$, $a_2 = b_2 = 3$, $c_1 = d_1 = c_2 = d_2 = c_3 = d_3 = 3$ and quarantine rates as given in Table 4.

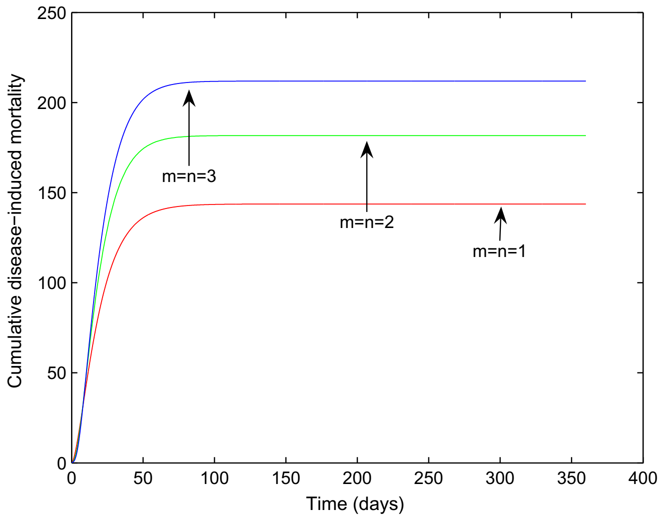

Fig. 6. Numerical simulations of the model (6) showing the cumulative number of disease-induced mortality for various disease stages ($m = n$). Parameter values used are as in Tables 2–4, with $\beta = 0.15$.

$\phi_2 = 0.1$, $\phi_3 = 0.20619$ were used in the simulations of the GD1 model (to account for the gradual refinement of quarantine and isolation), the values $\sigma_1 = \sigma_2 = \sigma_3 = 0.1$ and $\phi_1 = \phi_2 = \phi_3 = 0.20619$ were used in the simulations of the GD2 model (that is why the $\mathcal{R}_c$ value for the GD1 model is 0.9710, while that of the GD2 model is 0.7861 for this setting).

The effect of the distribution of sojourn times for the symptomatic period $(1/\kappa)$ is monitored by simulating the GD1 model (6) with the parameters in Table 2 for the case where the periods are either same or varied in each stage (i.e., the case where $d_j = n = c_j$ versus the case where $d_j \neq n \neq c_j$). In both cases, the same numerical simulation results were obtained (Fig. 9). In other words, distributing the average sojourn times equally or unequally between the sub stages of the symptomatic classes (I and H) does not alter the numerical simulation results obtained. The effect of the distribution of sojourn times in the asymptomatic classes (E and Q; given by $1/\alpha$) is also monitored by simulating the model with the parameters in Table 2 for three different scenarios. An asymptomatic period $1/\alpha = 6$ days is chosen, and distributed as follows:

(I) 2.5 days in E_1 and Q_1 classes (i.e., $1/a_1\alpha = 1/b_1\alpha = 2.5$ days), 2 days in E_2 and Q_2 classes (i.e., $1/a_2\alpha = 1/b_2\alpha = 2$ days) and 1.5 days in E_3 and Q_3 classes (i.e., $1/a_3\alpha = 1/b_3\alpha = 1.5$ days);

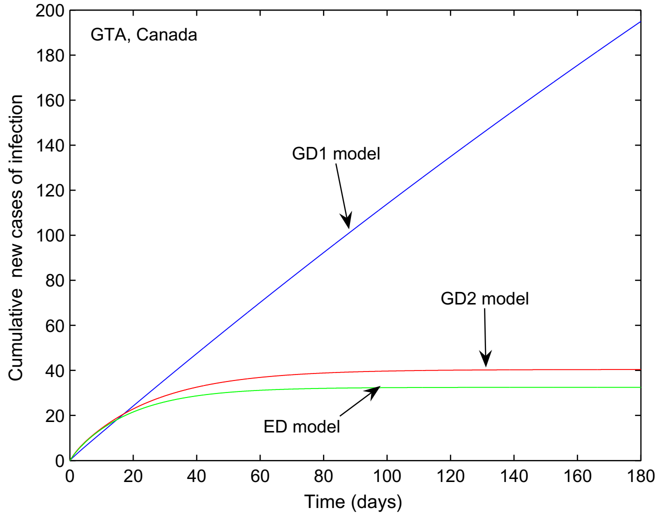

Fig. 7. Numerical simulations of the model (6) showing the cumulative number of probable SARS for the GTA generated using the GD1, GD2 and ED models. Parameter values used are as in Tables 2–4, with $\beta = 0.2$, $\psi = 0$. GD1 model: $m = n = 3$, GD2 model: $m = n = 3$; $\sigma_1 = \sigma_2 = \sigma_3 = 0.1$ and $\phi_1 = \phi_2 = \phi_3 = 0.20619$; ED model: $m = n = 1$.

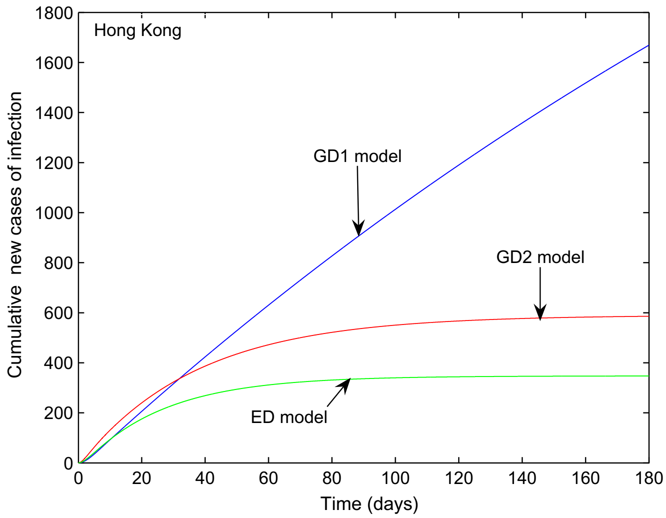

Fig. 8. Numerical simulations of the model (6) showing the cumulative number of probable SARS for the Hong Kong generated using the GD1, GD2 and ED models. Parameter values used are as in Tables 2–4, with $\beta = 0.2$, $\psi = 0$ and $\Pi = 122$. GD1 model: $m = n = 3$, GD2 model: $m = n = 3$; $\sigma_1 = \sigma_2 = \sigma_3 = 0.1$ and $\phi_1 = \phi_2 = \phi_3 = 0.20619$; ED model: $m = n = 1$.

(II) 2 days in E_1 and Q_1 classes (i.e., $1/a_1\alpha = 1/b_1\alpha = 2$ days), 2 days in E_2 and Q_2 classes (i.e., $1/a_2\alpha = 1/b_2\alpha = 2$ days) and 2 days in E_3 and Q_3 classes (i.e., $1/a_3\alpha = 1/b_3\alpha = 2$ days);

(III) 1.5 days in E_1 and Q_1 classes (i.e., $1/a_1\alpha = 1/b_1\alpha = 1.5$ days), 2 days in E_2 and Q_2 classes (i.e., $1/a_2\alpha = 1/b_2\alpha = 2$ days) and 2.5 days in E_3 and Q_3 classes (i.e., $1/a_3\alpha = 1/b_3\alpha = 2.5$ days).

The simulation results obtained (Fig. 10) clearly show that if the asymptomatic period is distributed such that more time is spent in the early stages of the asymptomatic (latent and quarantine) classes (i.e., more time is spent in E_1, E_2, Q_1, Q_2 classes in comparison to in E_3 and Q_3 classes), the cumulative number of new cases is higher than for the cases where the asymptomatic period is distributed equally among the stages or if more time is spent in the later asymptomatic stages. In other words, unlike for the case of the sojourn time spent in the symptomatic classes (I and H), the way the sojourn time is distributed in the asymptomatic compartments (E and Q) affects the cumulative number of new cases.

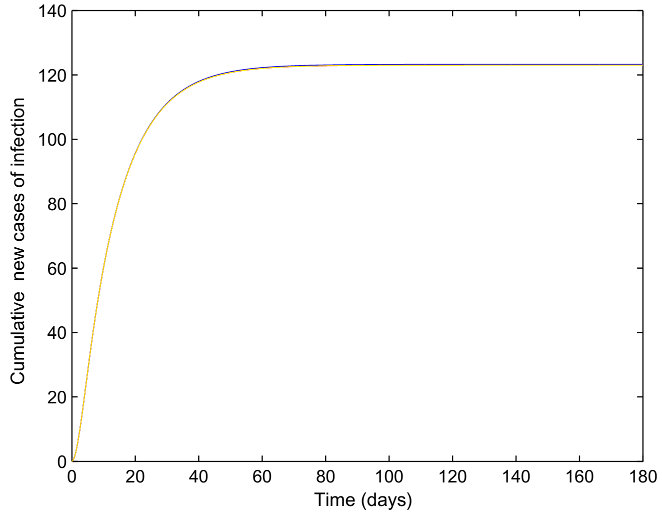

Fig. 9. Numerical simulations of the model (6) showing the cumulative number of new cases for various distributions of the symptomatic period $(1/\kappa)$ using different values of $c_1 = d_1$, $c_2 = d_2$, and $c_3 = d_3$. Parameter values used are as in Table 2, with $\beta = 0.2$, $\psi = 0$, $\sigma_1 = \sigma_2 = \sigma_3 = 0.1$ and $\phi_1 = \phi_2 = \phi_3 = 0.20619$.

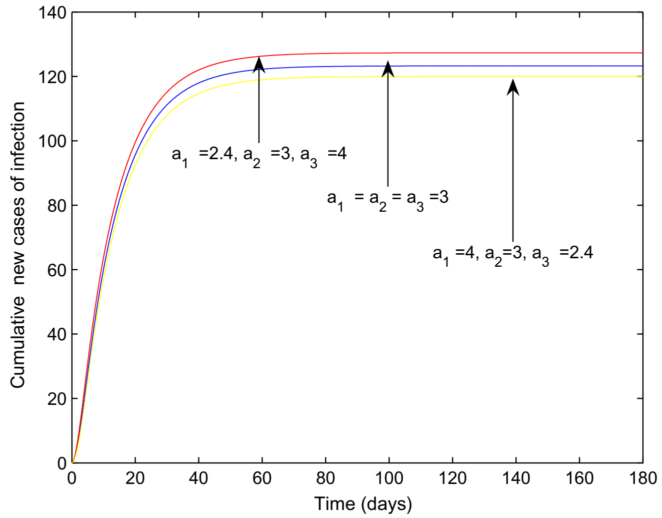

Fig. 10. Numerical simulations of the model (6) showing the cumulative number of new cases for various distributions of the asymptomatic period $(1/\alpha)$ using different values of $a_1 = b_1$, $a_2 = b_2$, and $a_3 = b_3$. Parameter values used are as in Table 2, with $\beta = 0.2$, $\psi = 0$, $\sigma_1 = \sigma_2 = \sigma_3 = 0.1$ and $\phi_1 = \phi_2 = \phi_3 = 0.20619$.

5. Conclusions

A new deterministic model for disease transmission, subject to the use of quarantine (of asymptomatic cases) and isolation (of individuals with disease symptoms), is presented and rigorously analyzed. The model, which is based on the assumption that the mean waiting periods in all infected classes obey a gamma distribution, adopts a standard incidence formulation for the infection rate. An important feature of this model is that it allows for equal or unequal distribution of the sojourn time in each of the associated infected compartment. Furthermore, it allows for the gradual refinement of quarantine and isolation measures (this was the case during the 2003 SARS outbreaks). The main theoretical findings of the study are given below:

(i) The model (6) has a globally-asymptotically stable disease-free equilibrium whenever the associated reproduction number $(\mathcal{R}_c)$ is less than unity.
(ii) The model has a unique endemic equilibrium whenever the reproduction number exceeds unity.
(iii) The unique endemic equilibrium of the model is shown to be globally-asymptotically stable for a special case.

Numerical simulations of the model (6), using data related to the 2003 SARS outbreaks, show the following:

(a) the cumulative number of new cases of infection decreases with increasing quarantine or isolation rate;
(b) the cumulative number of disease-related mortality increases with increasing number of disease stages (m and n);
(c) unlike the ED and GD2 models, the model (6) gives numerical results that are consistent with the 2003 SARS outbreaks data for the GTA and Hong Kong;
(d) distributing the average sojourn time equally or unequally between the respective symptomatic classes does not alter the numerical simulation result obtained (i.e., the cumulative number of new cases);
(e) if the asymptomatic period is distributed such that more time is spent in the early asymptomatic (latent and quarantine) stages, the cumulative number of new cases is higher than for the cases where the period is distributed equally among the asymptomatic stages or if more time is spent in the later asymptomatic stages.

Acknowledgments

One of the authors (ABG) acknowledges, with thanks, the support in part of the Natural Science and Engineering Research Council (NSERC) and Mathematics of Information Technology and Complex Systems (MITACS) of Canada. MAS gratefully acknowledges the support of the Institute of Industrial Mathematical Sciences and the University of Manitoba Graduate Fellowship. The authors are grateful to Alex Leblanc for helpful discussions on the formulation of the gamma distribution.

Appendix A. Properties of gamma distribution [12]

A random variable X that is gamma-distributed with scale θ and shape k is denoted by

$$X \sim \Gamma(k,\theta) \text{ or } X \sim \text{Gamma}(k,\theta).$$

Properties:

(i) **Summation**: if X_i has a $\Gamma(k_i,\theta)$ distribution for $i = 1,2,\ldots,N$, then $\sum_{i=1}^{N} X_i \sim \Gamma\left(\sum_{i=1}^{N} k_i,\theta\right)$ provided all X_i are independent.
(ii) **Scaling**: if $X \sim \Gamma(k,\theta)$ then for any $\alpha > 0$, $\alpha X \sim \Gamma\left(k,\frac{\theta}{\alpha}\right)$.

For example, we have $E_i \sim \Gamma(1,a_i\alpha)$ for $i = 1,2,\ldots,m$. It follows, from (ii), that $a_iE_i \sim \Gamma(1,\alpha)$. Similarly, $\frac{a_iE_i}{m} \sim \Gamma(1,m\alpha)$. Finally, by (i), we have $\sum_{i=1}^{m} \frac{a_iE_i}{m} \sim \Gamma(m,m\alpha)$.

Appendix B. Proof of Theorem 4

Proof. Consider the reduced model, given by (20) with (21). Let $\mathcal{R}_{cr} > 1$, so that the associated unique endemic equilibrium exists. Further, consider the following non-linear Lyapunov function:

$$\mathcal{F} = S - S^{**} - S^{**}\ln\left(\frac{S}{S^{**}}\right) + E_1 - E_1^{**} - E_1^{**}\ln\left(\frac{E_1}{E_1^{**}}\right) + \sum_{i=2}^{m} x_i\left[E_i - E_i^{**} - E_i^{**}\ln\left(\frac{E_i}{E_i^{**}}\right)\right] + \sum_{j=1}^{n} y_j\left[I_j - I_j^{**} - I_j^{**}\ln\left(\frac{I_j}{I_j^{**}}\right)\right],$$

where the coefficients x_i ($i = 1,\ldots,m$) and y_j ($j = 1,\ldots,n$) are positive constants to be determined. Thus,

$$\dot{\mathcal{F}} = \dot{S} - \frac{S^{**}}{S}\dot{S} + \dot{E}_1 - \frac{E_1^{**}}{E_1}\dot{E}_1 + \sum_{i=2}^{m} x_i\left(\dot{E}_i - \frac{E_i^{**}}{E_i}\dot{E}_i\right) + \sum_{j=1}^{n} y_j\left(\dot{I}_j - \frac{I_j^{**}}{I_j}\dot{I}_j\right).$$

Substituting the expressions of the derivatives from the system (20), using (21), gives (note that the relation $\Pi = \beta_1 S^{**}\sum_{j=1}^{n} I_j^{**} + \mu S^{**}$, at endemic steady-state, has been used)

$$\begin{aligned}\dot{\mathcal{F}} = {} & \beta_1 S^{**}\sum_{j=1}^{n} I_j^{**} + \mu S^{**} - \beta_1 S\sum_{j=1}^{n} I_j - \mu S - \beta_1\frac{S^{**}}{S}\sum_{j=1}^{n} I_j^{**} - \mu\frac{(S^{**})^2}{S} + \beta_1 S^{**}\sum_{j=1}^{n} I_j^{**} + \mu S^{**} + \beta_1 S\sum_{j=1}^{n} I_j - f_1E_1 - \beta_1 S\sum_{j=1}^{n}\frac{I_jE_1^{**}}{E_1}\\ & + f_1E_1^{**} + \sum_{i=2}^{m} x_ia_{i-1}\alpha E_{i-1} - x_if_iE_i - x_ia_{i-1}\alpha\frac{E_{i-1}E_i^{**}}{E_i} + x_if_iE_i^{**} + y_1a_m\alpha E_m - y_1f_{m+1}I_1 - y_1a_m\frac{E_mI_1^{**}}{E_m} + y_1f_{m+1}I_1^{**}\\ & + \sum_{j=2}^{n} y_jd_{j-1}\kappa I_{j-1} - y_jf_{m+j}I_j - y_jd_{j-1}\kappa\frac{I_{j-1}I_j^{**}}{I_j} + y_jf_{m+j}I_j^{**},\end{aligned}$$

which can simplified to

$$\dot{\mathcal{F}} = \mu S^{**}\left(2 - \frac{S^{**}}{S} - \frac{S}{S^{**}}\right) + \beta_1 S^{**}\sum_{j=1}^{n} I_j^{**} - \beta_1 \frac{S^{**}}{S}\sum_{j=1}^{n} I_j^{**} + \beta_1 S^{**}\sum_{j=1}^{n} I_j^{**} - \beta_1 S\sum_{j=1}^{n}\frac{I_j E_1^{**}}{E_1} + (x_2 a_1\alpha - k_1)E_1 + \sum_{i=2}^{m-1}(x_{i+1}a_i\alpha - x_i f_i)E_i + (y_1 a_m\alpha - x_m f_m)E_m + \sum_{j=1}^{n-1}(\beta_1 S^{**} + y_{j+1}d_j\kappa - y_j f_{m+j})I_j + (\beta_1 S^{**} - y_n f_{m+n})I_n + \sum_{i=2}^{m}\left(x_i f_i E_i^{**} - x_i a_{i-1}\alpha\frac{E_{i-1}E_i^{**}}{E_i}\right) - y_1 a_m\frac{E_m I_1^{**}}{I_1} + y_1 f_{m+1} I_1^{**} + \sum_{j=2}^{n}\left(y_j f_{m+j} I_j^{**} - y_j d_{j-1}\kappa\frac{I_{j-1}I_j^{**}}{I_j}\right). \quad (22)$$

The coefficients x_i ($i = 2,\ldots,m$) and y_j ($j = 1,\ldots,n$) are chosen such that

$$\begin{aligned} &x_2 a_1\alpha - k_1 = 0,\\ &x_{i+1}a_i\alpha - x_i f_i = 0; \quad \text{for } i = 3,\ldots,m-1,\\ &y_1 a_m\alpha - x_m f_m = 0,\\ &\beta_1 S^{**} + y_{j+1}d_j\kappa - y_j f_{m+j} = 0,\\ &\beta_1 S^{**} - y_n f_{m+n} = 0, \end{aligned} \quad (23)$$

so that, from (23),

$$\begin{aligned} &x_i = \prod_{l=1}^{i-1}\frac{f_l}{a_l\alpha}; \quad i = 2,\ldots,m,\\ &y_1 = \prod_{l=1}^{m}\frac{f_l}{a_l\alpha};\\ &y_n = \frac{\beta_1 S^{**}}{f_{m+n}}; \end{aligned} \quad (24)$$

and,

$$y_{n-j} = \frac{\beta_1 S^{**}}{f_{m+n-j}} + \beta_1 S^{**}\sum_{s=1}^{j}\frac{\prod_{l=s}^{j} d_{n-l}\kappa}{\prod_{l=s-1}^{j} f_{n+m-l}}; \quad j = 1,\ldots,n-2.$$

Using the relations (24) in Eq. (22) gives

$$\dot{\mathcal{F}} = \mu S^{**}\left(2 - \frac{S^{**}}{S} - \frac{S}{S^{**}}\right) + 2\beta_1 S^{**}\sum_{j=1}^{n} I_j^{**} - \beta_1\frac{S^{**}}{S}\sum_{j=1}^{n} I_j^{**} - \beta_1 S\sum_{j=1}^{n}\frac{I_j E_1^{**}}{E_1} - f_1\frac{E_1 E_2^{**}}{E_2} + \frac{f_1 f_2}{a_1\alpha}E_2^{**} + \sum_{i=3}^{m} - \frac{\prod_{l=1}^{i-1} f_l}{\prod_{l=1}^{i-2} a_l\alpha}\frac{E_{i-1}E_i^{**}}{E_i} + \frac{\prod_{l=1}^{i} f_l}{\prod_{l=1}^{i-1} a_l\alpha}E_i^{**} - \frac{\prod_{l=1}^{m} f_l}{\prod_{l=1}^{m-1} a_l\alpha}\frac{E_m I_1^{**}}{I_1} + \frac{\prod_{l=1}^{m+1} f_l}{\prod_{l=1}^{m} a_l\alpha}I_1^{**} + \sum_{j=2}^{n-1} - d_{j-1}\kappa\left(\frac{\beta_1 S^{**}}{f_{m+j}} + \beta_1 S^{**}\sum_{s=1}^{n-j}\frac{\prod_{l=s}^{n-j} d_{n-l}\kappa}{\prod_{l=s-1}^{n-j} f_{n+m-l}}\right)\frac{I_{j-1}I_j^{**}}{I_j} + \sum_{j=2}^{n-1} f_{m+j}\left(\frac{\beta_1 S^{**}}{f_{m+j}} + \beta_1 S^{**}\sum_{s=1}^{n-j}\frac{\prod_{l=s}^{n-j} d_{n-l}\kappa}{\prod_{l=s-1}^{n-j} f_{n+m-l}}\right)I_j^{**} - \frac{\beta_1 S^{**} d_{n-1}\kappa}{f_{m+n}}\frac{I_{n-1}I_n^{**}}{I_n} + \beta_1 S^{**} I_n^{**}. \quad (25)$$

It can be shown from (20) that, at endemic steady-state,

$$\begin{aligned} &f_1 = \frac{\beta_1 S^{**}\sum_{j=1}^{n} I_j^{**}}{E_1^{**}},\\ &\frac{\prod_{l=1}^{i} f_l}{\prod_{l=1}^{i-1} a_l\alpha} = \frac{\beta_1 S^{**}\sum_{j=1}^{n} I_j^{**}}{E_i^{**}} \quad i = 2,\ldots,m,\\ &\frac{\prod_{l=1}^{m+1} f_l}{\prod_{l=1}^{m} a_l\alpha} = \frac{\beta_1 S^{**}\sum_{j=1}^{n} I_j^{**}}{I_1^{**}} \end{aligned} \quad (26)$$

and,

$$\frac{d_j\kappa}{f_{m+j+1}} = \frac{I_{j+1}^{**}}{I_j^{**}} \quad j = 1,\ldots,n-1. \quad (27)$$

Using the relations in (26) and (27) in Eq. (25) gives

$$\dot{\mathcal{F}} = \mu S^{**}\left(2 - \frac{S^{**}}{S} - \frac{S}{S^{**}}\right) + (m+2)\beta_1 S^{**}\sum_{j=1}^{n} I_j^{**} - \beta_1 \frac{S^{**}}{S}\sum_{j=1}^{n} I_j^{**} - \beta_1 S \sum_{j=1}^{n}\frac{I_j E_1^{**}}{E_1} - \beta_1 S^{**}\sum_{j=1}^{n} I_j^{**}\left(\sum_{i=1}^{m-1}\frac{E_i E_{i+1}^{**}}{E_{i+1}^{**}E_i}\right) - \beta_1 S^{**}\frac{E_m I_1^{**}}{I_1^{**}E_m}$$
$$\times \sum_{j=1}^{n} I_j^{**} - \beta_1^{**} S^{**}\sum_{j=1}^{n-1}\left(\frac{I_j I_{j+1}^{**}}{I_{j+1}}\sum_{l=j+1}^{n}\frac{I_l^{**}}{I_j^{**}}\right) + \beta_1 S^{**}\sum_{j=2}^{n}\left(\sum_{l=j}^{n} I_l^{**}\right),$$

which can be re-written as

$$\dot{\mathcal{F}} = \mu S^{**}\left(2 - \frac{S^{**}}{S} - \frac{S}{S^{**}}\right) + \beta_1 S^{**}\left[(m+2) - \frac{S^{**}}{S} - \sum_{i=1}^{m-1}\frac{E_i E_{i+1}^{**}}{E_{i+1}^{**}E_i} - \frac{E_m I_1^{**}}{E_m^{**}I_1}\right] + \beta_1 S^{**}$$
$$\times \sum_{j=2}^{n} I_j^{**}\left[(m+j+1) - \frac{S^{**}}{S} - \sum_{i=1}^{m-1}\frac{E_i E_{i+1}^{**}}{E_{i+1}^{**}E_i} - \frac{E_m I_1^{**}}{E_m^{**}I_1} - \sum_{l=1}^{j-1}\frac{I_l I_{l+1}^{**}}{I_{l+1}I_l^{**}} - \frac{S I_j E_1^{**}}{S^{**}I_j^{**}E_1}\right]. \tag{28}$$

Finally, since the arithmetic mean exceeds the geometric mean, it follows that

$$\begin{aligned} &2 - \frac{S^{**}}{S} - \frac{S}{S^{**}} \leqslant 0,\\ &(m+2) - \frac{S^{**}}{S} - \sum_{i=1}^{m-1}\frac{E_i E_{i+1}^{**}}{E_{i+1}^{**}E_i} - \frac{E_m I_1^{**}}{E_m^{**}I_1} \leqslant 0, \end{aligned} \tag{29}$$

and,

$$(m+j+1) - \frac{S^{**}}{S} - \sum_{i=1}^{m-1}\frac{E_i E_{i+1}^{**}}{E_{i+1}^{**}E_i} - \frac{E_m I_1^{**}}{E_m^{**}I_1} - \sum_{l=1}^{j-1}\frac{I_l I_{l+1}^{**}}{I_{l+1}I_l^{**}} - \frac{S I_j E_1^{**}}{S^{**}I_j^{**}E_1} \leqslant 0 \quad \text{for } j = 2,\ldots,n. \tag{30}$$

Further, since all parameters of the model (6) are non-negative, it follows from (29) and (30), using (28), that $\dot{\mathcal{F}} \leqslant 0$ for $\mathcal{R}_{cr} > 1$. Hence, $\mathcal{F}$ is a Lyapunov function for the sub-system of the model (20) consisting of the equations for S, E_i ($i = 1,\ldots,m$), I_j ($j = 1,\ldots,n$) of the model (20) on $\mathcal{D}\setminus\mathcal{D}_0$. Therefore, by the LaSalle's Invariance Principle [9],

$$\begin{aligned} &\lim_{t\to\infty} S(t) = S^{**}, \quad \lim_{t\to\infty} E_i(t) = E_i^{**}, \quad \text{for all } i = 1,\ldots,m,\\ &\lim_{t\to\infty} I_j(t) = I_j^{**}, \quad \text{for all } j = 1,\ldots,n. \end{aligned} \tag{31}$$

It is clear from (31) that $\limsup_{t\to\infty} E_1 = E_1^{**}$. Thus, for sufficiently small $\varpi > 0$, there exists a constant $n_1 > 0$ such that $\limsup_{t\to\infty} E_1 \leqslant E_1^{**} + \varpi$ for all $t > n_1$. It follows from the $(m + n + 2)$th equation of the model (20) that, for $t > n_1$,

$$\dot{Q}_1 \leqslant \sigma_1(E_1^{**} + \varpi) - f_{m+n+1}Q_1.$$

Thus, by comparison theorem [26],

$$Q_1^{\infty} = \limsup_{t\to\infty} Q_1 \leqslant \frac{\sigma_1(E_1^{**} + \varpi)}{f_{m+n+1}},$$

so that, by letting $\varpi \to 0$,

$$Q_1^{\infty} = \limsup_{t\to\infty} Q_1 \leqslant \frac{\sigma_1 E_1^{**}}{f_{m+n+1}}. \tag{32}$$

Similarly (by using $\liminf_{t\to\infty} E_1 = E_1^{**}$), it can be shown that

$$Q_{1\infty} = \liminf_{t\to\infty} Q_1 \geqslant \frac{\sigma_1 E_1^{**}}{f_{m+n+1}}. \tag{33}$$

Thus, it follows from (32) and (33) that

$$Q_{1\infty} \geqslant \frac{\sigma E_1^{**}}{f_{m+n+1}} \geqslant Q_1^{\infty}.$$

Hence,

$$\lim_{t\to\infty} Q_1 = \frac{\sigma_1 E_1^{**}}{f_{m+n+1}} = Q_1^{**}. \tag{34}$$

Similarly, it can be shown that

$$\begin{aligned}
&\lim_{t\to\infty} Q_i(t) = Q_i^{**}, \quad \text{for all } i = 2,\ldots,m,\\
&\lim_{t\to\infty} H_j(t) = H_j^{**}, \quad \text{for all } j = 1,\ldots,n, \\
&\lim_{t\to\infty} R(t) = R^{**}.
\end{aligned} \tag{35}$$

Thus, by combining (31), (34) and (35), it follows that every solution to the equations of the reduced model, with initial condition in $\mathcal{D}\setminus\mathcal{D}_0$, approaches the unique endemic equilibrium of the reduced model (20) with (21) as $t\to\infty$ for $\mathcal{R}_{cr}>1$ and $\psi = 0$. $\square$

References

[1] R.M. Anderson, R.M. May, Population Biology of Infectious Diseases, Springer-Verlag, New York, 1982.
[2] G. Chowell, C. Castillo-Chavez, P. Fenimore, C. Kribs-Zaleta, L. Arriola, J. Hyman, Model parameters and outbreak control for SARS, EID 10 (2004) 1258–1263.
[3] G. Chowell, N.W. Hengartner, C. Castillo-Chavez, P.W. Fenimore, J.M. Hyman, The basic reproductive number of ebola and the effects of public health measures: the cases of Congo and Uganda, J. Theor. Biol. 1 (2004) 119–126.
[4] O. Diekmann, J.A.P. Heesterbeek, J.A.J. Metz, On the definition and computation of the basic reproduction ratio $\mathcal{R}_0$ in models for infectious disease in heterogeneous population, J. Math. Biol. 28 (1990) 365–382.
[5] C. Donnelly, A. Ghani, G. Leung, A. Hedley, C. Fraser, S. Riley, et al, Epidemiological determinants of spread of casual agent of severe acute respiratory syndrome in Hong Kong, Lancet 361 (2003) 1761–1766.
[6] M. Eichner, M. Schwehm, H. Duerr, S.O. Brockmann, The influenza pandemic preparedness planning tool InfluSim, BMC Infec. Dis. 7 (2007) 17.
[7] Z. Feng, D. Xu, H. Zhao, Epidemiological models with non-exponentially distributed disease stages and application to disease control, Bull. Math. Biol. 69 (2007) 1511–1536.
[8] A.B. Gumel et al, Modelling strategies for controlling SARS outbreaks, Proc. Roy. Soc. Ser. B 271 (2004) 2223–2232.
[9] J.K. Hale, Ordinary Differential Equations, John Wiley and Sons, New York, 1969.
[10] H.W. Hethcote, The mathematics of infectious diseases, SIAM Rev. 42 (2000) 599–653.
[11] H.W. Hethcote, M. Zhien, L. Shengbing, Effects of quarantine in six endemic models for infectious diseases, Math. Biosci. 180 (2002) 141–160.
[12] R.V. Hogg, A.T. Craig, Introduction to Mathematical Statistics, fourth ed., Macmillan, New York, 1978.
[13] Hong Kong in Figs. ed., Census and Statistics Department, Hong Kong Special Administrative Region, 2006.
[14] R.R. Kao, M.G. Roberts, Quarantine-based disease control in domesticated animal herds, Appl. Math. Lett. 4 (1998) 115–120.
[15] W.O. Kermack, A.G. McKenrick, A contribution to the mathematical theory of epidemics, Proc. Roy. Soc. Lond. 115 (1927) 700–721.
[16] W.O. Kermack, A.G. McKenrick, A contribution to the mathematical theory of epidemics, Part II, Proc. Roy. Soc. Lond. 138 (1932) 55–83.
[17] G. Leung et al, The epidemiology of severe acute respiratory syndrome in the 2003 Hong Kong epidemic: an analysis of all 1755 patients, Ann. Intern. Med. 9 (2004) 662–673.
[18] M. Lipsitch et al, Transmission dynamics and control of severe acute respiratory syndrome, Science 300 (2003) 1966–1970.
[19] J.O. Lloyd-Smith, A.P. Galvani, W.M. Getz, Curtailing transmission of severe acute respiratory syndrome within a community and its hospital, Proc. Roy. Soc. Lond. B 170 (2003) 1979–1989.
[20] R.G. McLeod, J.F. Brewster, A.B. Gumel, D.A. Slonowsky, Sensitivity and uncertainty analyses for a SARS model with time-varying inputs and outputs, Math. Biosci. Eng. 3 (2006) 527–544.
[21] C.N. Podder, A.B. Gumel, C.S. Bowman, R.G. McLeod, Mathematical study of the impact of quarantine, isolation and vaccination in curtailing an epidemic, J. Biol. Syst. 15 (2007) 185–202.
[22] S. Riley et al, Transmission dynamics of etiological agent of SARS in Hong Kong: the impact of public health interventions, Science 300 (2003) 1961–1966.
[23] R.A. Ross, The Prevention of Malaria, second ed., Murray, London, 1911.
[24] M.A. Safi, A.B. Gumel, Global asymptotic dynamics of a model for quarantine and isolation, Discrete Contin. Dyn. Syst. Ser. B 14 (2010) 209–231.
[25] O. Sharomi, C.N. Podder, A.B. Gumel, E. Elbasha, J. Watmough, Role of incidence function in vaccine-induced backward bifurcation in some HIV models, Math. Biosci. 2 (2007) 436–463.
[26] H.L. Smith, P. Waltman, The Theory of the Chemostat, Cambridge University Press, 1995.
[27] H.R. Thieme, Mathematics in Population Biology, Princeton University Press, 2003.
[28] P. van den Driessche, J. Watmough, Reproduction numbers and sub-threshold endemic equilibria for compartmental models of disease transmission, Math. Biosci. 180 (2002) 29–48.
[29] W. Wang, S. Ruanx, Simulating the SARS outbreak in Beijing with limited data, J. Theor. Biol. 227 (2005) 369–379.
[30] H.J. Wearing, P. Rohani, M.J. Keeling, Appropriate models for the management of infectious diseases, PLoS Med. 2 (2005) 621–627.
[31] G.F. Webb, M.J. Blaser, H. Zhu, S. Ardal, J. Wu, Critical role of nosocomial transmission in the Toronto SARS outbreak, Math. Biosci. Eng. 1 (2004) 1–13.
[32] X. Yan, Y. Zou, Optimal and sub-optimal quarantine and isolation control in SARS epidemics, Math. Comput. Model. 47 (2008) 235–245.
[33] Y. Yang, Z. Feng, D. Xu, Analysis of a model with multiple infectious stages and arbitrary distributed stage durations, Math. Model. Nat. Phenom. 3 (2008) 180–193.